JGR Space Physics

RESEARCH ARTICLE
10.1029/2018JA026018

**Key Points:**
- MSTIDs observed at conjugate locations in the Europe-Africa longitude sector for the first time
- Direction of propagation of Sutherland MSTIDs is mostly westward, consequence of its large magnetic declination
- Propagation speeds are larger at Sutherland due to weaker Earth's magnetic field and its configuration at this longitude sector

**Supporting Information:**
- Supporting Information S1
- Movie S1
- Movie S2
- Movie S3
- Movie S4

**Correspondence to:**
C. Martinis,
martinis@bu.edu

**Citation:**
Martinis, C., Baumgardner, J., Mendillo, M., Wroten, J., MacDonald, T., Kosch, M., et al. (2019). First conjugate observations of medium-scale traveling ionospheric disturbances (MSTIDs) in the Europe-Africa longitude sector. *Journal of Geophysical Research: Space Physics*, *124*, 2213–2222. https://doi.org/10.1029/2018JA026018

Received 4 SEP 2018
Accepted 20 JAN 2019
Accepted article online 31 JAN 2019
Published online 25 MAR 2019



# First Conjugate Observations of Medium-Scale Traveling Ionospheric Disturbances (MSTIDs) in the Europe-Africa Longitude Sector

**Carlos Martinis[1], Jeffrey Baumgardner[1], Michael Mendillo[1], Joei Wroten[1], Timothy MacDonald[1], Michael Kosch[2], Monica Lazzarin[3], and Gabriele Umbriaco[3]**

[1]Center for Space Physics, Boston University, Boston, Massachusetts, USA, [2]South African National Space Agency, Cape Town, South Africa, [3]Department of Physics and Astronomy, University of Padua, Padua, Italy

**Abstract** All-sky imagers located in Asiago, Italy (45.87°N, 11.53°E; 40.7° magnetic latitude) and Sutherland, South Africa (32.37°S, 20.81°E; −40.7° magnetic latitude) are used to study magnetically conjugate medium scale traveling ionospheric disturbances (MSTIDs). We present initial results from the first year of joint Asiago-Sutherland data sets from July 2016 to June 2017. The 630.0-nm airglow perturbations showing different kinds of waves were frequently observed. Some of these wave events resemble MSTIDs propagating south-westward in Asiago, typical direction observed at other longitude sectors in the northern hemisphere. They are mostly observed as single bands propagating through the field of view of the all-sky imagers. We select and analyze five cases of magnetically conjugate bands associated with MSTIDs. The bands observed at Sutherland move mainly westward, noticeably different from the north-west direction of propagation of MSTIDs observed in the southern hemisphere. We compare the MSTIDs propagation speeds and find that three cases show larger values at Sutherland. When we compare the zonal speeds all the cases show larger values at Sutherland. On average, the propagation speed at Sutherland is 20% larger and the zonal speed is ~35% larger. The westward motion at Sutherland is explained by taking onto account how its magnetic declination (~24°W) affects the orientation of the bands. The larger speed at Sutherland is due to the weaker Earth's magnetic field in the southern hemisphere and the particular configuration of the magnetic field lines in this longitude sector.

## 1. Introduction

Medium-scale traveling ionospheric disturbances (MSTIDs) is the term used to identify propagating band-like structures in the ionosphere at low and midlatitudes. The term was coined when ionosonde observations detected the presence of oscillatory patterns in ionospheric parameters that had periods on the order of 0.5 to ~2 hr and wavelengths around 100–200 km (Hunsucker, 1982). These structures were observed in daytime or nighttime propagating in all directions. In the late 1990s, the first optical observations of nighttime MSTIDs were performed at the Arecibo Observatory (Mendillo et al., 1997). One of the characteristics of these structures was that they showed a consistent south-westward motion in the northern hemisphere. Subsequent observations in the Australian sector (Otsuka et al., 2004) and in the American sector (Martinis et al., 2006) showed that in the southern hemisphere they move north-westward

In the Asian sector, Shiokawa et al. (2003) showed that nighttime MSTIDs occurred more frequently during local summer and in general were not accompanied by strong spread *F* signatures. In the American sector Martinis et al. (2010) showed that in addition to the main peak in local summer, as observed in the Japanese sector, there was a similar peak in local winter. This study complemented the study of Garcia et al. (2000) who had shown peak occurrence during local summer, although no winter observations were available.

In addition to MSTIDs studies using ASIs, radio measurements have also provided valuable information on their seasonal characteristics. Kotake et al. (2007) showed a main peak of occurrence during local summer, with a smaller secondary peak in the local winter in western United States. More recently, a study by Otsuka et al. (2013), using GPS total electron content data in Europe, showed statistical results indicating peak occurrence of nighttime MSTIDs during the December solstice with a very small secondary peak in the June solstice, contrary to the results shown in the American and Asian sectors. The Otsuka et al. (2013) study does not agree with the results presented by Hernández-Pajares et al. (2006) who showed only a peak

occurrence of MSTIDs during June solstice in the year 2002 using six GPS stations in Europe, and no peak in local winter.

Significant theoretical work has been done to understand nighttime MSTIDs properties. Originally they were related to the Perkins instability (Perkins, 1973). This theory seemingly provides the right geometry for the alignment and direction of propagation. Bands were aligned NW-SE and the instability would maximize in the NE or SW quadrants. Further analysis indicated that the growth rate was too small and that the waves generated by the instability should propagate in the NE direction, contrary to the observations (Kelley, 2009). This allowed the inclusion of additional mechanisms necessary to explain the generation and evolution of MSTIDs. During the early 2000s simulations taking into account the coupling between structuring and instabilities in the *E* region with the *F* region were conducive to reproduce the proper conditions for MSTIDs generation and direction of propagation (Cosgrove & Tsunoda, 2004; Makela & Otsuka, 2012; Tsunoda, 2006; Yokoyama, 2014; Yokoyama et al., 2009). Thus, the current state of the art of our knowledge of MSTIDs involves the interaction between *E* region structures and the *F* region. The results from Martinis et al. (2010) showing a strong peak of occurrence during local winter suggested that weaker magnetic fields due to the South Atlantic magnetic anomaly in the opposite hemisphere or the presence of stronger *E* region perturbations in the opposite hemisphere could lead to increased activity in the local winter hemisphere. In order to explain the local winter peak in the European sector, Otsuka et al. (2013) pointed out that in addition to strong *E* region activity, other factors should be involved in the growth of the instabilities.

Conjugate observations of MSTIDs were presented for the first time by Otsuka et al. (2004). They showed MSTIDs occurring simultaneously at conjugate locations, a fact that reflects the complex interaction involving the mapping of electric fields from one hemisphere to another in order to maintain the cohesive behavior of structures occurring thousands of kilometers apart. Martinis et al. (2011) showed conjugate MSTIDs in the American sector with the typical south-westward (north-westward) propagation in the northern (southern) hemisphere. In addition they used GPS measurements to show the presence of weak phase scintillations as measured by computing the rate of change of total electron content.

An aspect that has been not carefully studied is the precise direction of propagation of the MSTIDs. It is common to read in the published literature that, in the northern hemisphere, MSTIDs propagate south-westward while in the southern hemisphere they propagate north-westward. The theoretical studies predict that the wave vector of the instability (perpendicular to the frontal phase of the bands) makes an angle of ~30$^{o}$ with the magnetic east direction (Behnke, 1979; Kelley, 2009). After geometrical considerations this condition is equivalent to have the propagation vector making a ~30$^{o}$ angle with the local magnetic meridian. Then, when the magnetic declination is close to zero the bands will move in the directions typically observed.

We present here the first results using all-sky imagers operating at magnetically conjugate locations in Italy and South Africa. These imagers are part of the network of instruments deployed by the Boston University imaging group (Martinis et al., 2017). As we will show below, the main results of this study are (a) while the typical NE–SW propagation holds for the northern hemisphere observations, the motion of the southern hemisphere conjugate structures is mostly westward, not SE-NW as observed at other longitudes, and (b) the Southern Hemisphere structures seem to move ~20% faster than the conjugate structures observed in the Northern Hemisphere (although two out of the five cases show similar values). This hemispheric difference is even larger when the zonal component of the propagation speed is compared (with the five individual cases analyzed having larger speeds in the Southern Hemisphere), resulting on structures moving on average ~35% faster in the Southern Hemisphere.

## 2. First Conjugate Point Observations in Europe and South Africa

The first low-light-level, all-sky imaging system using a CCD detector to operate continuously in Western Europe was field-tested successively at the University of Padua's observatory in Asiago, Italy, in 2010, with operations beginning in April 2011. The Asiago all-sky imager (ASI) uses a set of four narrowband filters to observe structures in the ionosphere and mesosphere (see instrument description in Martinis et al. (2017)). Past studies using Asiago observations of 630.0-nm emission described stable auroral red arcs (Baumgardner et al., 2013; Mendillo et al., 2012, 2013) that appear at subauroral latitudes during geomagnetic storms.

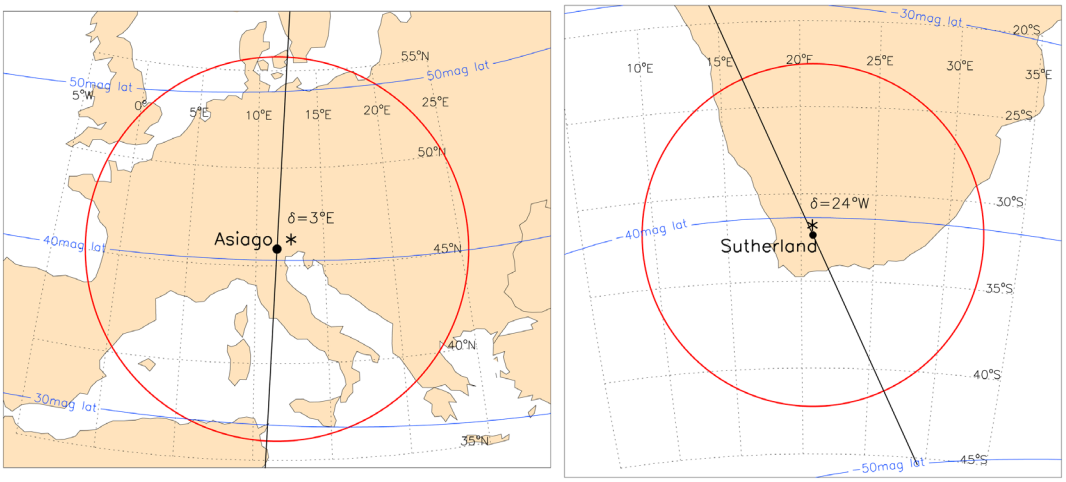


**Figure 1.** (left) Fields of view (FOV) in geographic coordinates for the all-sky-imagers at Asiago, Italy and (right) its conjugate point location in Sutherland, South Africa. The circles give FOV for zenith angles $0^{o}$–$80^{o}$ for 630.0-nm emission from an airglow layer at 300 km. The dots mark the locations of zenith at each site, with asterisks showing the mapped zenith locations of the corresponding conjugate points. Solid black lines show magnetic declination.

Observations of the mesosphere are recorded using filters for OH ($\lambda > 695.0$ nm) and atomic oxygen ($\lambda = 557.7$ nm). Recent findings about mesospheric bore events are described in Smith et al. (2017). Here we use images at 630.0 nm to conduct our first optical study of MSTIDs over Europe, together with a companion set of images from an identical instrument at its geomagnetic conjugate point, in South Africa.

The Asiago Observatory is located at 45.87°N and 11.53°E. Its quasi-dipole (QD) magnetic coordinates (Richmond, 1995) are 40.68°N, 87.09°E. The geomagnetic field line at zenith at 300 km extends to a distance above the geomagnetic equator (called apex height) of 1.82 Earth radii from the center of the Earth (denoted as L = 1.82). A geomagnetic conjugate point is defined as the continuation of that L = 1.82 field line into the southern hemisphere where it reaches 300 km at 32.31°S and 20.31°E. The South African Astronomical Observatory at Sutherland (32.37°S, 20.81°E) is remarkably close to the Asiago conjugate point, and a second all-sky-imager was established there in July 2016. The ASI at the South African Astronomical Observatory uses the same set of filters as used in Asiago plus 589.3 nm (Na) and 777.4 nm (OI). ASI observations started at Sutherland in mid-July 2016, and analysis of the first year of joint Asiago-Sutherland data sets is now possible (July 2016 to June 2017).

Figure 1 shows the field of view of the all-sky imagers at Asiago and Sutherland for 630.0-nm emission at 300 km. While the astronomical observatories at Asiago and Sutherland were established to maximize observations of faint celestial targets, the meteorological and seeing conditions for the Asiago location have deteriorated considerably since its founding in 1942. The encroachment of city lights has reduced a once dark-sky environment, and yet scientific quality all-sky images can still be obtained using narrowband filters (~1.8 nm) with state-of-the-art CCD detectors. At the South African Astronomical Observatory, light pollution is nearly zero, and seeing conditions are excellent, thus same-night conjugate point case studies are essentially determined by the availability of data from Asiago.

In the first 12 months of joint observations (12 July 2016 to 30 June 2017), a total of 326 nights of data were available for Asiago and 334 for Sutherland. Only two nights per month were excluded due to full moon conditions. The percentage of those nights being clear or mostly clear (mostly clear being those nights that were not photometric but clear enough to see airglow features in the presence of clouds) totaled 58% at Asiago and 76% at Sutherland. This 12-month period did not include a noteworthy set of solar-terrestrial disturbances. The average solar flux was characterized by $<F_{10.7}> = 79.8$ units, indicative of solar-minimum conditions.

The most frequent departures from uniform airglow were associated with activity attributed to *F* region gravity waves and MSTIDs. On virtually every clear night, dynamical patterns of moving airglow structures appear in an airglow image. The observed modulations in brightness are very subtle, in general less than ~10%. These are confirmed as ionospheric structures and not tropospheric features, that is, clouds, or

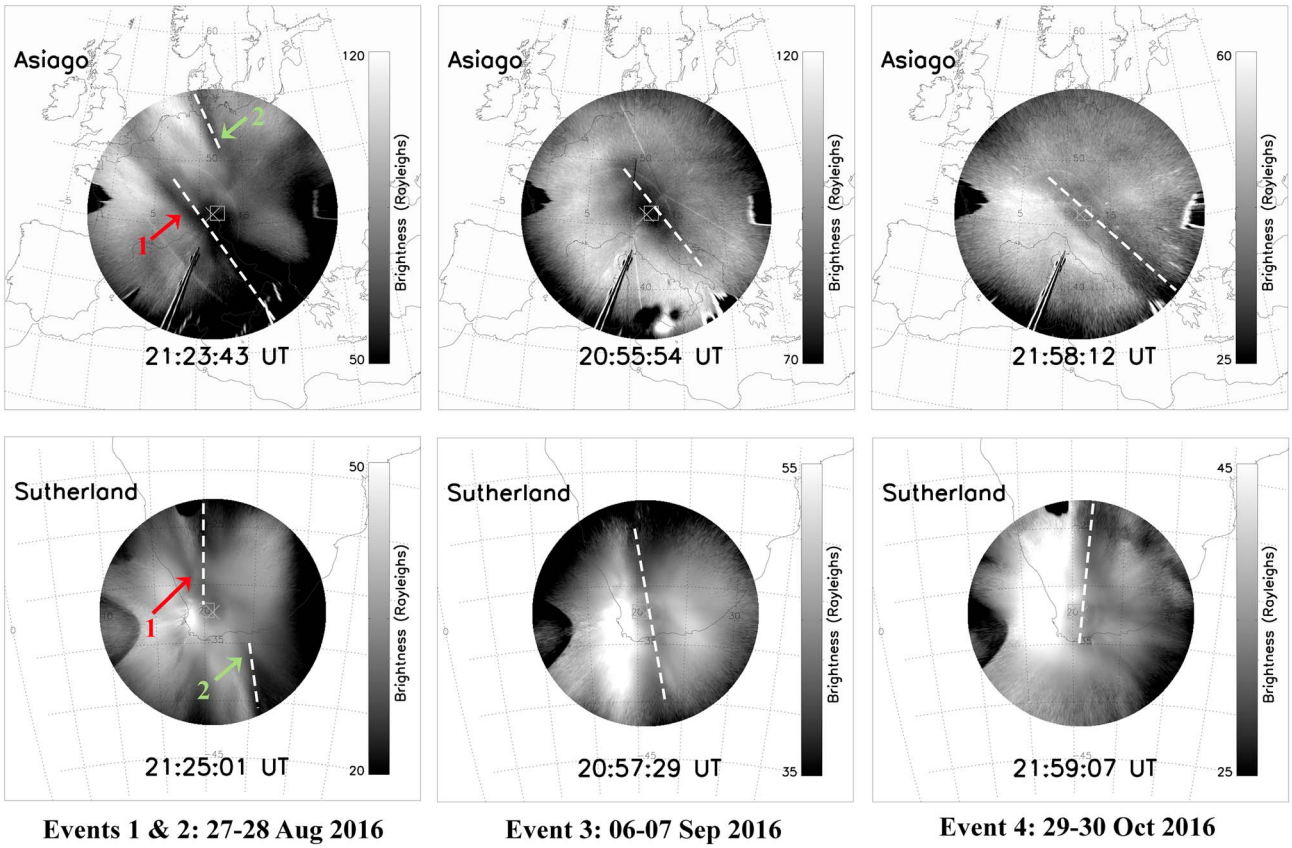


**Figure 2.** Examples of bands observed at (top) Asiago and (bottom) Sutherland corresponding to events 1, 2 (on the same night; left), 3 (center), and 4 (right). The bands at Asiago are tilted northwest-southeast, while the ones at Sutherland are mainly in the north-south direction. White dashed lines are superimposed to indicate the structures representing the dark bands that were studied.

leakage through the 630.0-nm filter (from other nightglow emissions related to mesospheric wave activity) by using images at off-band wavelengths (605.0 nm in both sites). The MSTIDs do not show large brightness variations nor the typical multicycle band-like structures routinely observed in the American and Japanese sectors.

During this first year of joint observations 39 nights (out of 189) showed dynamical events at Asiago and 88 nights (out of 254) at Sutherland. These events are thus twice more likely to be seen at Sutherland than at Asiago. This factor of 2 difference might simply be due to the Sutherland site having more clear nights (34% versus 20%); a better statistical summary awaits additional years of observations and analysis.

The wave events identified exhibited different directions of propagation—consistent with expectations of diverse local gravity wave activity in the thermosphere above each site. In general, we do not expect to observe conjugate signatures from these waves. A subset of wave activity at Asiago revealed large-scale dark patterns that propagated from the northeast to the southwest, the classic signature of MSTIDs in the northern hemisphere. For these events at Asiago, we then examined the same nights at Sutherland.

## 3. Case-Study Events

We identified four nighttime data sets for detailed study in this paper. For the Europe-Africa longitude sector, nighttime hours span two days of universal time (UT), and thus, observations can start at ~18:00 UT on day 1 and conclude at ~06:00 UT on day 2. We define an event as the presence of a dark band associated with MSTIDs that can be observed at both sites. Events 1 and 2 occurred on 27–28 August 2016, with event 3 on 6–7 September 2016, event 4 on 29–30 October 2016, and event 5 on 30–31 October 2016. Examples of conjugate bands from events 1–2, 3, and 4 are shown in Figure 2, with the top images from Asiago and the ones at

the bottom from Sutherland. Movies for the nights showing events 3 and 4 are provided in the supporting information. The structures observed are very weak and do not appear well defined as those observed in the American and Japanese sectors. Dashed white lines are drawn to help in the identification of the dark conjugate structures.

### 3.1. Imaging Processing

Each of the ASI systems uses a filter wheel that contains four to six narrow wavelength bands (~1.8 nm) centered on atmospheric emissions of interest, and one for control images to assess the presence of tropospheric clouds and background light. Integration times of 2 min are used and thus the sequence of images at a given wavelength is separated by approximately 7 min at Asiago and ~11 min at Sutherland. Each image is corrected for detector effects, as well as for contamination of background light (Milky Way, stars, and light pollution) by use of the off-band image closest in time. Calibration to brightness units of Rayleighs (R) is achieved by using a set of known stellar brightness values within each field of view. Finally, observations using an all-sky lens portray physical space in a "warped" fashion, that is, considerable spatial compression at large zenith angles. For an assumed centroid of emission for 630.0-nm airglow at 300 km, each pixel (with its unique zenith angle and azimuth) is mapped to a geographic grid—with the result called an "unwarped" image. Full details of the image processing protocols used for the Boston University ASI network are given in Baumgardner et al. (2013) and Martinis et al. (2017).

### 3.2. Velocities and Directions of Propagation

Using the full sets of all-sky-images in unwarped format (as shown in Figure 2), the procedure for determining the speed and direction of propagation of bands associated with MSTIDs was as follows. Typically, images are unwarped to have geographic north at the top assuming a height of 300 km. A vertical (meridional), 10-pixel-wide scan is taken down the middle of an image and averaged to an 800 × 1 array. This 800-pixel-long sample of brightness versus latitude pertains to a single image time. Subsequent images spaced at approximately 7 min at Asiago and 11 min at Sutherland are then stacked to fill a latitude versus time array. The same process is used with 10-pixel-wide scans taken horizontally (zonal) across the middle of the image to create an array of brightness on a grid of longitude versus time. We call the resultant meridional and zonal versus time arrays "velograms" (Martinis et al., 2003). In each velogram the band is identified and its speed and direction of propagation can be calculated by measuring the slope of the line representing the projection of the motion of the MSTID as it crosses the central column (zonal velogram) and central row (meridional velogram). To measure the slope of a given band, the endpoints were selected manually and connected to give an initial guess of the line from which a slope can be computed. For each pixel on this line, the darkest pixel within a vertical range of ±7 pixels centered on the initial guess is found, and a new, least squares fit line to these pixel coordinates is used to calculate the slope. Uncertainties are calculated from both the uncertainty in the slope measurements as well as the uncertainty caused by the assumed map scale (km/pixel).

Figure 3 gives an example of a velogram for event 3 on the night of 6–7 September 2016. Asiago results are shown on the left panel while Sutherland results are displayed on the right panel. For each station, the top panel shows the zonal velogram and the bottom panel the meridional velogram. At Asiago the red lines between 20 and 21 UT are used to calculate the slopes. Similarly, at Sutherland the slopes are computed near 21 UT. Once the slopes of the dark band on the velograms are measured, they are used to obtain two components of the velocity that are the projections of the MSTIDs speed on the central column and row of the images, $V'_m$ and $V'_z$, respectively, not directly the meridional and zonal speeds. The angle of propagation is calculated as $\tan\theta = V'_m/V'_z$. The propagation speed V of the MSTIDs is obtained from $1/V^2 = 1/V'^2_m + 1/V'^2_z$. The true zonal, $V_z$, and meridional, $V_m$, components are $V_z = V\sin\theta$ and $V_m = V\cos\theta$. The results of the velogram analysis for the five events at both sites are summarized in Table 1. For each event, the speeds and their azimuths are shown for each station, with the last column showing the difference in the two azimuths or directions of propagation, that is, $\Delta\theta = \theta_{Sut} - \theta_{Asi}$. The average speeds and angles of propagation are shown in the last row. The average speeds of propagation at Sutherland are about 20% faster than at Asiago, but we notice that only three out of the five cases show Sutherland speeds larger than Asiago. The average azimuth of wave propagation at Asiago (~229°) is nearly the anticipated value of 225° for pure southwestard motion. For Sutherland, the anticipated motion toward the northwest would have azimuth around 315°, but the observed direction is considerably different, ~278°, a value that is nearly due west

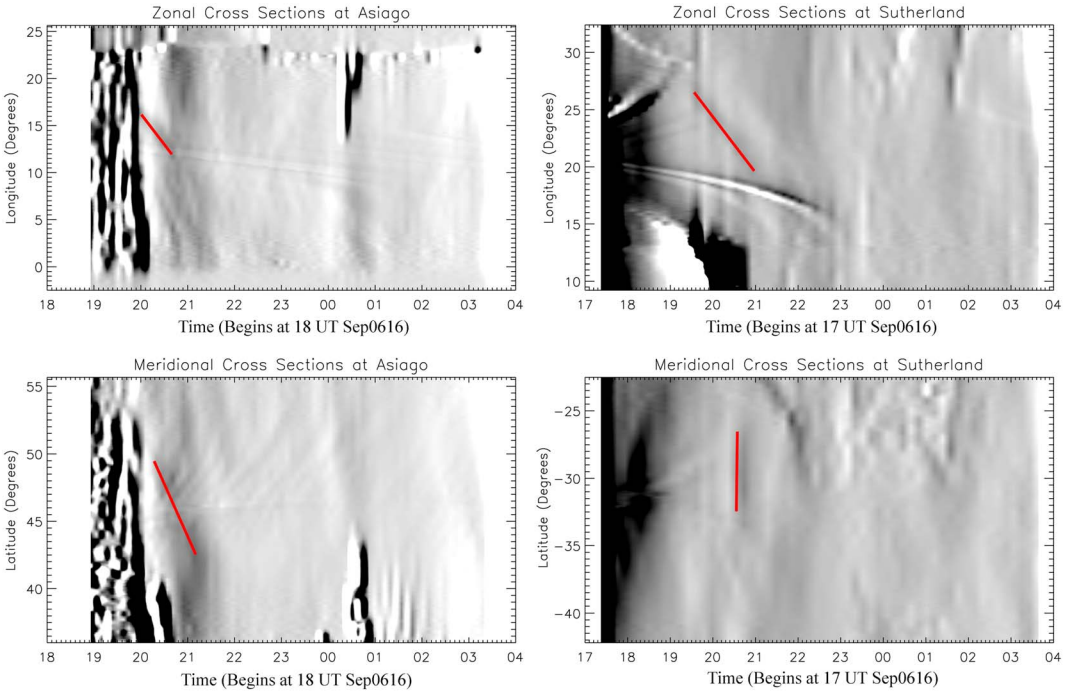


**Figure 3.** (top) Zonal and (bottom) meridional cuts for (left) Asiago and (right) Sutherland during the 6–7 September 2016 (event 3). The event appears as a dark band, indicated with red lines. The spatial and temporal patterns of those lines are used to derive wave speeds and directions (see text). Clouds in Asiago are observed from 19 UT to ~ 20 UT. The Asiago meridional scan also shows the presence of waves moving poleward throughout the night. For the zonal scan at Sutherland, the streaking from left to right results from residuals of the milky way not fully subtracted.

(270°). The events show an average $\Delta\theta = 44^{o}$. The day when the difference in azimuth is the largest (57°) corresponds to the day where the equatorial geomagnetic index *Dst* reached −57 nT. A weak geomagnetic disturbance might have had an effect on the azimuth, something worth to investigate, but out of the scope of this paper. A graphical summary of the results shown in Table 1 appears in Figure 4 as compass plots. The left panel shows the velocity vectors for Asiago for the five events analyzed. The arrows show a clear south-westward motion with velocities varying from ~5 to ~116 m/s. The right panel shows a similar plot for the Sutherland events. The direction of propagation is clearly strongly westward, a surprising result considering that one would have expected a north-westward propagation as shown in the published literature of southern hemisphere MSTIDs. The speeds in the southern hemisphere are between ~93 and 166 m/s.

## 4. Discussion

ASIs operating at magnetically conjugate locations have recorded the occurrence of waves and MSTIDs during the period July 2016 to June 2017. The peak occurrence of Sutherland MSTIDs is during

**Table 1**
*Summary of MSTID Speeds and Azimuths of the Five Events Analyzed in This Study for Both Sites*

| | Asiago | | | Sutherland | | | |
|---|---|---|---|---|---|---|---|
| Event | Speed (m/s) | Zonal speed (m/s) | Azimuth (°) | Speed (m/s) | Zonal speed (m/s) | Azimuth (°) | Δ Azimuth (°) |
| 1 (27–28 Aug 16) | 85 ± 2 | 65 ± 3 | 230 ± 1 | 93 ± 7 | 93 ± 7 | 273 ± 1 | 43 |
| 2 (27–28 Aug 16) | 116 ± 4 | 97 ± 5 | 237 ± 1 | 108 ± 18 | 107 ± 18 | 278 ± 1 | 41 |
| 3 (6–7 Sep 16) | 97 ± 2 | 78 ± 3 | 234 ± 1 | 128 ± 7 | 127 ± 7 | 262 ± 1 | 28 |
| 4 (29–30 Oct 16) | 99 ± 5 | 62 ± 7 | 219 ± 2 | 94 ± 10 | 93 ± 10 | 275 ± 1 | 57 |
| 5 (30–31 Oct 16) | 115 ± 8 | 84 ± 10 | 227 ± 2 | 168 ± 11 | 166 ± 11 | 277 ± 1 | 50 |
| Average | 102 ± 11 | 77 ± 13 | 229 ± 3 | 118 ± 25 | 117 ± 25 | 273 ± 2 | 44 |

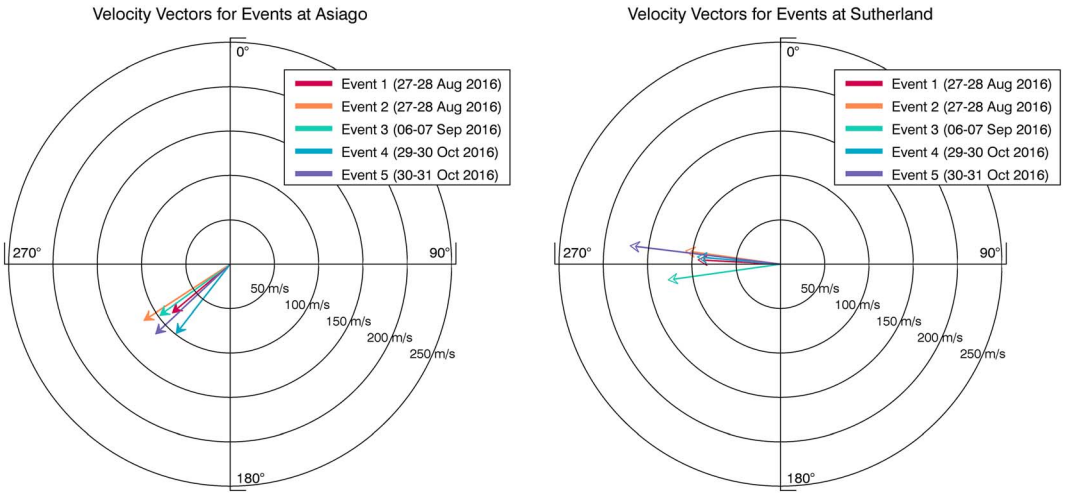


**Figure 4.** Vector representations of speeds and azimuth for MSTIDs at (left) Asiago and (right) Sutherland. Asiago results clearly show that the MSTIDs propagate in a direction between 210° and 240°, that is, southwestward, while at Sutherland they propagate mainly westward, that is, around 270°.

December solstice, while Asiago does not show MSTIDs peaking in a particular season. The Sutherland result agrees with past studies of MSTIDs occurrence rates in the southern hemisphere (Martinis et al., 2010). The Asiago result does not agree with the results from Otsuka et al. (2013), who showed peak occurrence rate during December solstice. Our statistical result is based on only one year of observations and on a reduced number of nights due to cloudiness conditions, and thus, it does not allow us to provide conclusive evidence of its validity. We will wait for multiyear observations to perform and obtain a better statistics.

We have presented five cases of simultaneous observations of MSTIDs. While the ones observed in the northern hemisphere show the typical southwestward motion, the ones at Sutherland move primarily in the westward direction. The average speed of the MSTIDs is larger in the Southern Hemisphere, but this result needs to be validated with more case studies to provide statistically meaningful conclusions. Figure 5 shows the average velocity vectors for the five events at each site. In this plot the magnetic field declination angles for zenith at both sites (red line for Asiago and green line for Sutherland) are also indicated. The difference in magnetic declination between the two sites is substantial, almost 30°. The large magnetic declination at Sutherland might be the cause of the almost-westward motion of the MSTIDs. This can be explained by recalling the conditions at midlatitudes that can lead to an instability in the *F* region. A plasma layer at midlatitudes can be supported against gravity by a southward wind or an eastward electric field (Perkins, 1973). If an eastward wind or northward electric field is present, the equilibrium is broken and the system is unstable. The growth rate due to a northward electric field is found to be proportional to sin $\alpha$ * sin ($\phi - \alpha$), where $\phi$ is the angle between the total electric field and magnetic east direction and $\alpha$ is the angle between the **k** vector of the wave and magnetic east direction (Garcia et al., 2000; Shiokawa et al., 2003). The theoretical analysis and numerical simulations show that the maximum growth rate occurs if $\alpha = \phi/2$ and unstable **k** vectors are either in the NE or SW quadrants in the northern hemisphere, or NW and SE in the southern hemisphere (Behnke, 1979). The bands associated with MSTIDs are perpendicular to the $\phi/2$ direction. The efficient direction for generation and propagation of waves triggered by the Perkins instability or by combined Perkins and *E* region instabilities is usually ~20–30° from the magnetic meridian (Garcia et al., 2000; Kelley, 2009; Perkins, 1973; Shiokawa et al., 2003). This fact could then explain why MSTIDs at Sutherland tend to move mainly westward, instead of north-westward. The magnetic declination at Asiago is very small, only 3°E, meaning that the ~ 30° tilt with respect to the magnetic meridian puts the frontal phases moving to the SW quadrant, or between ~210° and 240°. The magnetic declination at Sutherland is 24°W; therefore, the motion should be toward ~250° and 290°, that is, toward the west. This asymmetry could be easily removed if the motions were considered in a magnetic coordinate reference system. Past studies have always stated that MSTIDs moved north-westward (south-westward) in the southern

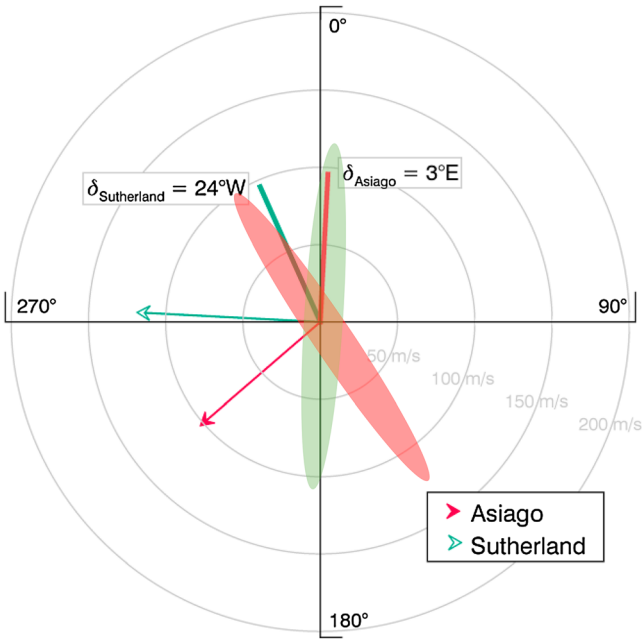


**Figure 5.** Average velocity vectors for Asiago (red arrow) and Sutherland (green arrow). Also shown are the magnetic declinations at both sites (green line, Sutherland; red line, Asiago). The colored ovals represent bands oriented ~30° with respect to magnetic meridian at each site.

(northern) hemisphere. There are no studies investigating precise directions of propagation at places with different magnetic declinations. For example, Garcia et al. (2000) showed that MSTIDs at Arecibo, where magnetic declination is 10°W, had a southwestward motion with angles of propagation of ~235°–240°. More recently, Takeo et al. (2017) used 16 years of ASI data over Shigaraki, Japan (where magnetic declination is 7°W), to show that MSTIDs moved primarily southwestward, that is, between ~215° and 240°. Figueiredo et al. (2018) studied 10 nights with MSTIDs in Cachoeira Paulista (where magnetic declination is 21 W) and concluded that they moved north-westward, although their Figure 4 shows almost-westward motion in most of them (in agreement with our explanation).

Another result obtained here shows that the propagation speed is on average larger by ~20% in the southern hemisphere. This difference originates basically from three of the cases shown in Table 1 (events 1, 3, and 5). No studies comparing magnetically conjugate speeds of MSTIDs have been published to date. This is our first attempt to do this with a limited number of cases. The velocity of a wave originated by a Perkins instability-like process is the $(E \times B)/B^2$ drift component parallel to $\mathbf{k}_\perp$ (Kelley, 2009). The larger values at Sutherland could be attributed to the presence of the South Atlantic magnetic anomaly. In this region the magnetic field is very weak: using the IGRF-12 model (Thébault et al., 2015), its intensity at 300 km at Sutherland is 23,800 nT, while at its conjugate point, near Asiago, is 41,400 nT, a difference of ~40%. Then one could expect larger drifts in the southern hemisphere. This effect has been observed when comparing zonal drifts from the motion of irregularities associated with equatorial spread-*F* events using GPS techniques in the American sector, where zonal velocities were found to be ~30% larger in the southern hemisphere (Sobral et al., 2009). A significant difference in the configuration of the Earth's magnetic field exists between the American and African sectors. In the South American sector, low-magnitude field values are due to field lines stretched apart (i.e., separated) mainly in the longitudinal direction, whereas over South Africa the magnetic field lines are stretched apart more in the latitudinal direction (Laundal & Richmond, 2017). As a consequence, in South America, the main differences when comparing speeds in both hemispheres exist for the zonal speeds, while in the African sector the main difference is for the meridional speeds. This could explain why a 20% difference in the MSTID total velocity could exist, even though the magnetic field intensity at Sutherland is ~40% weaker than the intensity at Asiago. The MSTIDs at Sutherland are moving mainly westward, so no strong meridional component exists. When we compare the zonal speeds at both sites, all the events show that the Sutherland structures move faster than the Asiago structures, on average 35% faster.

It remains to be investigated why the brightness variations related to MSTIDs observed at Asiago and Sutherland are so weak and why they do not resemble well-formed band-like wave structures. This is in contrast with observations in the Japanese and American sectors, where MSTIDs are clearly identified as banded multiwavelength structures, with percentage variations in airglow brightness reaching 20–30%. A fact that could help to explain the weak brightness variations and bands not well formed is that the magnetic inclination angles of the two stations used in this study are large, between 60 and 65°. This value is close to the limit value found in the Otsuka et al. (2013) study, who found that MSTIDs were not present in Europe at geographic latitudes higher than 55° (~62° magnetic inclination). The studies in the Japanese sector involved ASIs located at stations with smaller magnetic inclination, around 45–50°, similar to those studies in the American sector that involved station with magnetic inclination around 40–45°. A large magnetic inclination means that the vertical component of the $E \times B/B^2$ is small and it cannot produce significant upward or downward perturbations in the *F* region. In addition, if one explains the origin of MSTIDs based on the coupling between the *F* region and *E* region structuring, that is, $E_s$ layers, wind shear in the *E* region does not produce strong $E_s$ layer under large magnetic inclination at midlatitude conditions.

## 5. Summary

All-sky imagers located in Asiago, Italy, and Sutherland, South Africa, are used to study magnetically conjugate MSTIDs. Asiago cloudy conditions render a limited number of clear skies during the first year of data presented here. At Sutherland, conditions are much better, with almost no pollution and a larger number of nights with clear skies. During the first year of operations airglow perturbations showing different kinds of wave activity were observed frequently. Some of these wave events resemble MSTIDs propagating southwestward in the Asiago ASI. The five cases analyzed here showed that the corresponding magnetic conjugate bands observed in the southern hemisphere at Sutherland tend to move mainly in the westward direction. The large magnetic declination at Sutherland indicates that the frontal bands should be oriented almost in the geodetic north-south direction with a direction of propagation perpendicular to the front, that is, mostly geodetic westward. The large magnetic inclination at both sites could be the cause of weak and not well-defined banded structures, contrary to the observations in the American and Japanese sectors. A comparison of the speeds of propagation shows that three out of the five cases move faster at Sutherland (~20% on average). When the zonal velocities are compared we observe that the five events show faster values at Sutherland (~35% on average). The anomalously weaker magnetic field in the southern hemisphere and its particular configuration above South Africa could be responsible for the higher speeds observed. Further analysis including more simultaneous cases is needed to provide statistical significance to justify the larger speeds observed at Sutherland.

**Acknowledgments**
This work was supported by grants from the National Science Foundation (AGS-1552301, C.M.; AGS-1123222, M. M.; and AGS-1552045, J.B.). We thank Dominique Pautet from Utah State University for the useful discussions on the interpretation of velograms/keograms and the calculation of zonal and meridional velocities. C.M. wishes to acknowledge the continuing assistance from the personnel of the Asiago and Sutherland Observatories. Data used in this work are available at www.buimaging.com.

## References

Baumgardner, J., Wroten, J., Mendillo, M., Martinis, C., Barbieri, C., Umbriaco, G., et al. (2013). Imaging space weather over Europe. *Space Weather*, *11*, 69–78. https://doi.org/10.1002/swe.20027

Behnke, R. (1979). *F* layer height bands in the nocturnal ionosphere over Arecibo. *Journal of Geophysical Research*, *84*(A3), 974–978. https://doi.org/10.1029/JA084iA03p00974

Cosgrove, R. B., & Tsunoda, R. T. (2004). Instability of the *E-F* coupled nighttime midlatitude ionosphere. *Journal of Geophysical Research*, *109*, A04305. https://doi.org/10.1029/2003JA010243

Figueiredo, C. A. O. B., Takahashi, H., Wrasse, C. M., Otsuka, Y., Shiokawa, K., & Barros, D. (2018). Investigation of nighttime MSTIDS observed by optical thermosphere imagers at low latitudes: Morphology, propagation direction, and wind filtering. *Journal of Geophysical Research: Space Physics*, *123*, 7843–7857. https://doi.org/10.1029/2018JA025438

Garcia, F. J., Kelley, M. C., Makela, J. J., & Huang, C.-S. (2000). Airglow observations of mesoscale low-velocity traveling ionospheric disturbances at midlatitudes. *Journal of Geophysical Research*, *105*(A8), 18,407–18,415. https://doi.org/10.1029/1999JA000305

Hernández-Pajares, M., Juan, J. M., & Sanz, J. (2006). Medium-scale traveling ionospheric disturbances affecting GPS measurements: Spatial and temporal analysis. *Journal of Geophysical Research*, *111*, A07S11. https://doi.org/10.1029/2005JA011474

Hunsucker, R. D. (1982). Atmospheric gravity waves generated in the high-latitude ionosphere: A review. *Reviews of Geophysics*, *20*(2), 293–315. https://doi.org/10.1029/RG020i002p00293

Kelley, M. C. (2009). *The Earth's Ionosphere: Plasma Physics and Electrodynamics*. Singapore: Academic 834 Press.

Kotake, N., Otsuka, Y., Ogawa, T., Tsugawa, T., & Saito, A. (2007). Statistical study of medium-scale traveling ionospheric disturbances observed with the GPS networtks in Southern California. *Earth, Planets and Space*, *59*(2), 95–102. https://doi.org/10.1186/BF03352681

Laundal, K. M., & Richmond, A. (2017). Magnetic coordinate systems. *Space Science Reviews*, *206*(1-4), 27–59. https://doi.org/10.1007/s11214-016-0275-y

Makela, J., & Otsuka, Y. (2012). Overview of nighttime ionospheric instabilities at low- and mid-latitudes: Coupling aspects resulting in structuring at the mesoscale. *Space Science Reviews*, *168*(1-4), 419–440. https://doi.org/10.1007/s11214-011-9816-6

Martinis, C., Baumgardner, J., Smith, S. M., Colerico, M., & Mendillo, M. (2006). Imaging science at El Leoncito, Argentina. *Annales Geophysicae*, *24*(5), 1375–1385. https://doi.org/10.5194/angeo-24-1375-2006

Martinis, C., Baumgardner, J., Wroten, J., & Mendillo, M. (2010). Seasonal dependence of MSTIDs obtained from 630.0 nm airglow imaging at Arecibo. *Geophysical Research Letters*, *37*, L11103. https://doi.org/10.1029/2010GL043569

Martinis, C., Baumgardner, J., Wroten, J., & Mendillo, M. (2011). All-sky imaging observations of conjugate medium-scale traveling ionospheric disturbances in the American sector. *Journal of Geophysical Research*, *116*, A05326. https://doi.org/10.1029/2010JA016264

Martinis, C., Baumgardner, J., Wroten, J., & Mendillo, M. (2017). All-sky-imaging capabilities for ionospheric space weather research using geomagnetic conjugate point observing sites. *Advances in Space Research*, *61*(7), 1636–1651. https://doi.org/10.1016/j.asr.2017.07.021

Martinis, C., Eccles, J. V., Baumgardner, J., Manzano, J., & Mendillo, M. (2003). Latitude dependence of zonal plasma drifts obtained from dual-site airglow observations. *Journal of Geophysical Research*, *108*(A3), 1129. https://doi.org/10.1029/2002JA009462

Mendillo, M., Barbieri, C., Baumgardner, J., Wroten, J., Cremonese, G., & Umbriaco, G. (2012). A stable auroral red arc over Europe. *Astronomy & Geophysics*, *53*, 16–18.

Mendillo, M., Baumgardner, J., Nottingham, D., Aarons, J., Reinisch, B., Scali, J., & Kelley, M. (1997). Investigations of thermospheric-ionospheric dynamics with 6300-Å images from the Arecibo observatory. *Journal of Geophysical Research*, *102*(A4), 7331–7343. https://doi.org/10.1029/96JA02786

Mendillo, M., Baumgardner, J., Wroten, J., Martinis, C., Smith, S., Merenda, K.-D., et al. (2013). Imaging magnetospheric boundaries at ionospheric heights. *Journal of Geophysical Research: Space Physics*, *118*, 2681–2693. https://doi.org/10.1002/jgra.50104

Otsuka, Y., Shiokawa, K., Ogawa, T., & Wilkinson, P. (2004). Geomagnetic conjugate observations of medium-scale traveling ionospheric disturbances at midlatitude using all-sky airglow imagers. *Geophysical Research Letters*, *31*, L15803. https://doi.org/10.1029/2004GL020262

Otsuka, Y., Suzuki, K., Nakagawa, S., Nishioka, M., Shiokawa, K., & Tsugawa, T. (2013). GPS observations of medium-scale traveling ionospheric disturbances over Europe. *Annales de Geophysique*, *31*(2), 163–172. https://doi.org/10.5194/angeo-31-163-2013

Perkins, F. (1973). Spread *F* and ionospheric currents. *Journal of Geophysical Research*, *78*(1), 218–226. https://doi.org/10.1029/JA078i001p00218

Richmond, A. D. (1995). Ionospheric Electrodynamics Using Magnetic Apex Coordinates. *Journal of Geomagnetism and Geoelectricity*, *47*(2), 191–212. https://doi.org/10.5636/jgg.47.191

Shiokawa, K., Otsuka, Y., Ihara, C., Ogawa, T., & Rich, F. J. (2003). Ground and satellite observations of nighttime medium-scale traveling ionospheric disturbance at midlatitude. *Journal of Geophysical Research*, *108*(A4), 1145. https://doi.org/10.1029/2002JA009639

Smith, S. M., Stober, G., Jacobi, C., Chau, J. L., Gerding, M., Mlynczak, M. G., et al. (2017). Characterization of a double mesospheric bore over Europe. *Journal of Geophysical Research: Space Physics*, *122*, 9738–9750. https://doi.org/10.1002/2017JA024225

Sobral, J. H. A., Abdu, M. A., Pedersen, T. R., Castilho, V. M., Arruda, D. C. S., Muella, M. T. A. H., et al. (2009). Ionospheric zonal velocities at conjugate points over Brazil during the COPEX campaign: Experimental observations and theoretical validations. *Journal of Geophysical Research*, *114*, A04309. https://doi.org/10.1029/2008JA013896

Takeo, D., Shiokawa, K., Fujinami, H., Otsuka, Y., Matsuda, T. S., Ejiri, M. K., et al. (2017). Sixteen year variation of horizontal phase velocity and propagation direction of mesospheric and thermospheric waves in airglow images at Shigaraki, Japan. *Journal of Geophysical Research: Space Physics*, *122*, 8770–8780. https://doi.org/10.1002/2017JA023919

Thébault, E., Finlay, C. C., Beggan, C. D., Alken, P., Aubert, J., Barrois, O., et al. (2015). International geomagnetic reference field: The 12th generation. *Earth, Planets and Space*, *67*(1), 79. https://doi.org/10.1186/s40623-015-0228-9

Tsunoda, R. (2006). On the coupling of layer instabilities in the nighttime midlatitude ionosphere. *Journal of Geophysical Research*, *111*, A11304. https://doi.org/10.1029/2006JA011630

Yokoyama, T. (2014). Hemisphere-coupled modeling of nighttime medium-scale traveling ionospheric disturbances. *Advances in Space Research*, *54*(3), 481–488. https://doi.org/10.1016/j.asr.2013.07.048

Yokoyama, T., Hysell, D. L., Otsuka, Y., & Yamamoto, M. (2009). Three-dimensional simulation of the coupled Perkins and $E_s$-layer instabilities in the nighttime midlatitude ionosphere. *Journal of Geophysical Research*, *114*, A03308. https://doi.org/10.1029/2008JA013789